Open Access

Journal of Energy and Power Technology

LIDSEN Publishing Inc.

Original Research

Thermodynamic and Structural Optimization of Organic Rankine Cycle Plant for Clean Energy Access Using Artificial Bee Colony and Multi-Criteria Decision-Making Algorithms

Aniebiet D. Udoh [1], Ogheneruona E. Diemuodeke [1,*], Mohammed M. Ojapah [1,*], Fidelis I. Abam [2], Joseph C. Ofodu [1]

1. Energy and Thermofluid Research Group, Department of Mechanical Engineering, Faculty of Engineering, University of Port Harcourt, PMB 5323, Choba, Port Harcourt, Rivers State, Nigeria; E-Mails: aniet2dave@yahoo.com; ogheneruona.diemuodeke@uniport.edu.ng; mohammed.ojapah@uniport.edu.ng; joseph.ofodu@uniport.edu.ng
2. Energy, Exergy and Environmental Research Group (EEERG), Department of Mechanical Engineering, University of Calabar, Calabar, Cross River State, Nigeria; E-Mail: fidelisabam@unical.edu.ng

* **Correspondences:** Ogheneruona E. Diemuodeke and Mohammed M. Ojapah; E-Mails: ogheneruona.diemuodeke@uniport.edu.ng; mohammed.ojapah@uniport.edu.ng

Academic Editor: Xiaolin Wang

Journal of Energy and Power Technology
2023, volume 5, issue 2
doi:10.21926/jept.2302015

Received: December 29, 2022
Accepted: March 30, 2023
Published: April 13, 2023

Abstract

The quest to decarbonize the energy space to avert the negative climate change consequences calls for using low/zero-carbon energy conversion technologies in the energy generation space. The Organic Rankine Cycle is a low/zero-carbon energy conversion technology for recovering waste heat from low to medium-temperature heat sources and for biomass conversion. Therefore, this paper presents the thermodynamic optimization, with an artificial bee colony algorithm, of different ORC configurations, including simple organic Rankine cycle, Regenerative Organic Rankine Cycle, Cascade Organic Rankine Cycle, Organic Rankine Cycle with Superheat, Organic Rankine Cycle with Superheat and Reheat, Regenerative-Superheat Organic Rankine Cycle, Regenerative-Reheat Organic Rankine Cycle and Two Complementary ORC using twelve (12) different working fluids. The thermodynamic

optimization was followed by structural optimization using a multi-criteria decision approach. The modified-TOPSIS multi-criteria decision-making analysis was used to perform the structural optimization. The overall optimization study shows that the Regenerative-Reheat Organic Rankine Cycle, operating with an isopentane of 0 GWP and ODP, was selected as the best ORC configuration. The Regenerative-Reheat Organic Rankine Cycle has the following performance; thermal efficiency of 49.5%, maximum power output of 0.4 MW, condenser pressure of 90 kPa, and turbine pressure of 3.37 MPa. The results presented in this work will support clean energy developers in the clean energy access sector, especially in the agrarian community with huge agro-waste generation potentials.

Keywords
Organic Rankine cycle; optimization; low-carbon energy; artificial bee colony; TOPSIS

1. Introduction

In response to the Paris Agreement, reached in 2015, many nations have begun to chart development pathways away from climate-forcing activities; where the oil and gas sector dominates in the energy space [1]. The quest to decarbonize the energy space to avert the negative climate change consequences calls for using low/zero-carbon energy conversion technologies in the energy generation space [2]. Renewable energy systems are typically termed zero-carbon (clean) energy conversion technologies, namely solar, wind, biomass and others.

Sub-Saharan Africa (SSA), Nigeria, for example, has the potential to substantially solve its energy needs through renewable energy sources [3]. Nigeria alone produces 1.5 million tons/year of rice husks, 1.6 million tons/year of maize cobs and 1.2 million tons/year of groundnut husks which form mountains of waste that expose communities to pests and fire hazards. At the same time, the same communities are among the most energy-poor communities in the world, having no access to good quality cooking fuel [4]. A potential way to curb the environmental hazard associated with agro-waste and the insufficient supply of electricity is the utilization of agro-wastes for power generation. The use of biomass for power generation is considered a green energy source since its use does not result in a net increase in the atmospheric content of CO_2 through proper forest management [5]. Also, investment in the production and utilization of biomass (the agro waste in this case) is an investment in food production [6]. The organic Rankine cycle is a widely used energy conversion technology for biomass to electricity [7].

The organic Rankine cycle (ORC) is a low to medium-grade thermal conversion technology that uses a much lower boiling point organic fluid than water, instead of the conventional Rankine cycle [8]. The ORC plant is well suited for biomass-to-power plants [9, 10], the chemical energy in the biomass is converted to internal energy, which is then converted to electricity via a series of energy conversion processes [7, 11]. The ORC is a well-established technology for decentralized power generation up to 10 MW [12], which renders the conventional steam Rankine cycle technically and economically unattractive. Three basic methods of converting the rice husk into useful energy are gasification, bio-digestion and direct combustion. The technology for gasification is not well proven,

with few available commercial projects with high investment costs [13], coupled with low cold energy efficiency [14]; the direct combustion of rice husk is a well-established technology [11].

Several Organic Rankine Cycle power plants are already in use [15]. Ref. [16] presented a study on a dual-loop Organic Rankine Cycle (ORC) to utilize waste heat from an internal combustion diesel engine using R245fa and R134a as working fluids. However, the optimization of the sizes and topologies of these plants is the thrust of this project. An optimum size is necessary for a given power generation capacity to minimize material and labour cost. The procedure for obtaining the plant size involves identifying the optimum sizes of the components of the ORC for the expected power output from the plant, identifying the optimum layout of the system components and selecting preferred parameters.

Ebrahimi [17] stated that the working fluid selected for an ORC profoundly impacts its performance characteristics. Several organic compounds have been experimented with and their efficiency determined as working fluids for ORC, including R245fa [17], Toluene, Xylene, n-pentane, n-butane, R-11, and R-22 [18]. These working fluids are classified as wet, dry or isentropic based on their thermodynamic diagrams at saturation regions. The slope of wet fluids is positive, dry fluids are negative, while isentropic fluids have a vertical curve. Ebrahimi [17] noted that wet working fluids could cause damage to turbine blades due to fluid condensation. The dry working fluids do not experience fluid condensation during the expansion that can damage the blades of the turbine and do not require superheat and are, therefore more commonly used in ORC systems. According to McMahan [18], a number of the physical properties of the working fluid are more important than the thermodynamic properties, such as thermal stability, toxicity, flammability and cost. However, the thermodynamic properties of interest of ORC working fluids include the vapor-specific volume which determines the size of the condensing equipment, and the saturation temperature, which determines the turbine design because of the need for superheat and the turbine inlet pressure.

Saffari et al. [19] applied the Artificial Bee Colony (ABC) algorithm to optimize a geothermal system operating on the Kalina power cycle. This algorithm, they noted, has been applied in two- and three-objective function multi-modal problems. Dervis Karaboga invented the ABC algorithm; it performs better in local and global optimums due to the reduced number of control parameters allowed.

The methods for multi-criteria decision-making include the Weighted Sum Method (WSM), Technique for Order Preference by Similarity to Ideal Solution (TOPSIS) and Preference Ranking Organization Method for Enrichment Evaluation (PROMETHEE), Analytical Hierarchy Process (AHP), Elimination et Choice Translating Reality (ELECTREE), Preference Ranking Organization Method for Enrichment Evaluation (PROMETHEE), Grey Incidence Method (GIM) [20, 21].

A multi-criteria decision-making model based on the fuzzy set was presented by Wang et al. [21]. They highlighted the place of human subjectiveness in assigning values to imprecise criteria, resulting in the use of fuzzy theory. Selected criteria of interest were grouped into technical, economic, social and environmental attributes, each having sub-groups. At the same time, four alternatives of Stirling engine, gas turbine, gas engine and solid oxide fuel cell were considered. Therefore, the present work combined the artificial bee colony and modified TOPSIS decision-making algorithms to perform the thermodynamic and structural optimization of eight organic Rankine cycles operating under different working fluids to support energy developers in the clean energy access sector.

2. Materials and Method

2.1 Description of System

The configurations of ORC for which the optimum parameters are desired are presented in the following subsections.

2.1.1 Simple Organic Rankine Cycle (SORC)

The configuration of SORC, shown in Figure 1, is the basic form of the ORC. It consists of a pump, condenser, turbine and evaporator. Cyclohexane, Benzene and Toluene can be used as working fluids in this cycle [22].

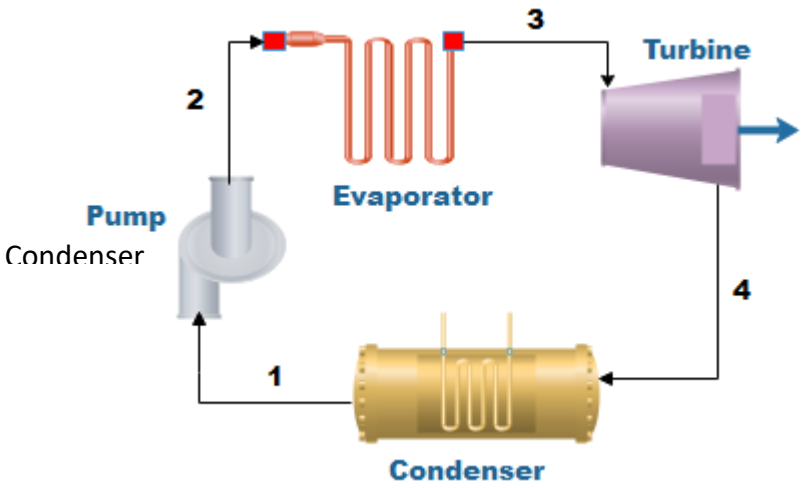

Figure 1 Structure of SORC.

2.1.2 Organic Rankine Cycle with Superheat (ORCS)

This configuration of ORC has a superheater installed between the evaporator and the turbine to allow pure gas into the turbine and prevent corrosion of the turbine blades. The block diagram of the plant is shown in Figure 2.

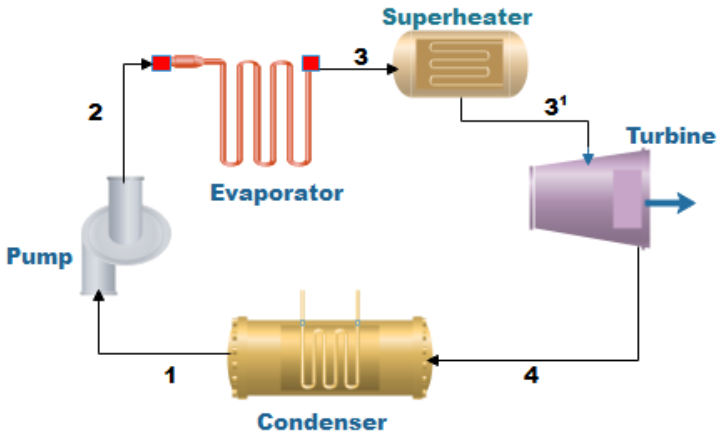

Figure 2 Structure of ORCS.

2.1.3 Organic Rankine Cycle with Superheat and Reheat (ORCSR)

The structure of ORCSR has a superheater and more than one turbine in the expansion process to utilize high and low-superheated working fluid and prevent corrosion of the turbine blades. The block diagram of the plant is shown in Figure 3.

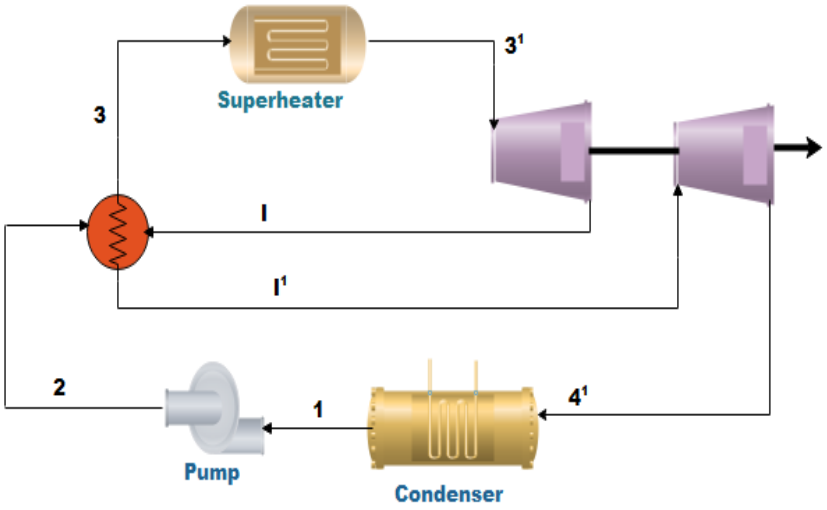

Figure 3 Structure of ORCR.

2.1.4 Regenerative Organic Rankine Cycle (RORC)

The RORC structure has an additional component, a regenerator between the turbine outlet and the evaporator inlet, to the SORC. Its structure is shown in Figure 4. The essence of the regenerator is to recover a part of the internal energy exiting the turbine and reduce the heat load of the condenser.

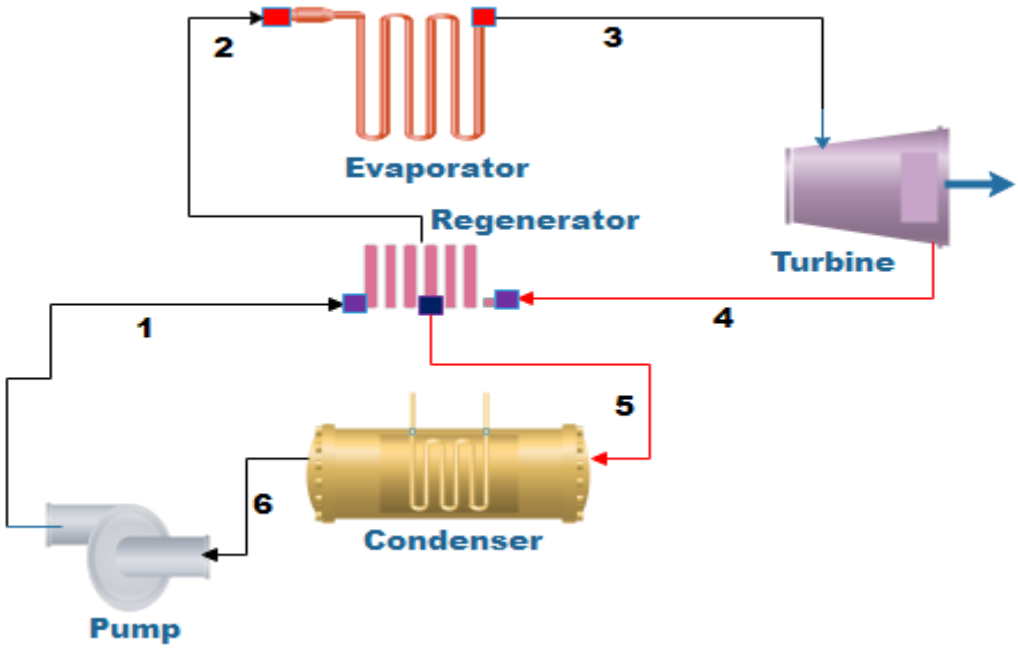

Figure 4 Structure of RORC.

2.1.5 Cascade Organic Rankine Cycle (CORC)

The cascade ORC structure comprises at least two stages, where the first stage evaporator acts as the condenser of the immediate next stage. Consequently, various configurations of the CORC exist; the simplest form of this configuration is shown in Figure 5.

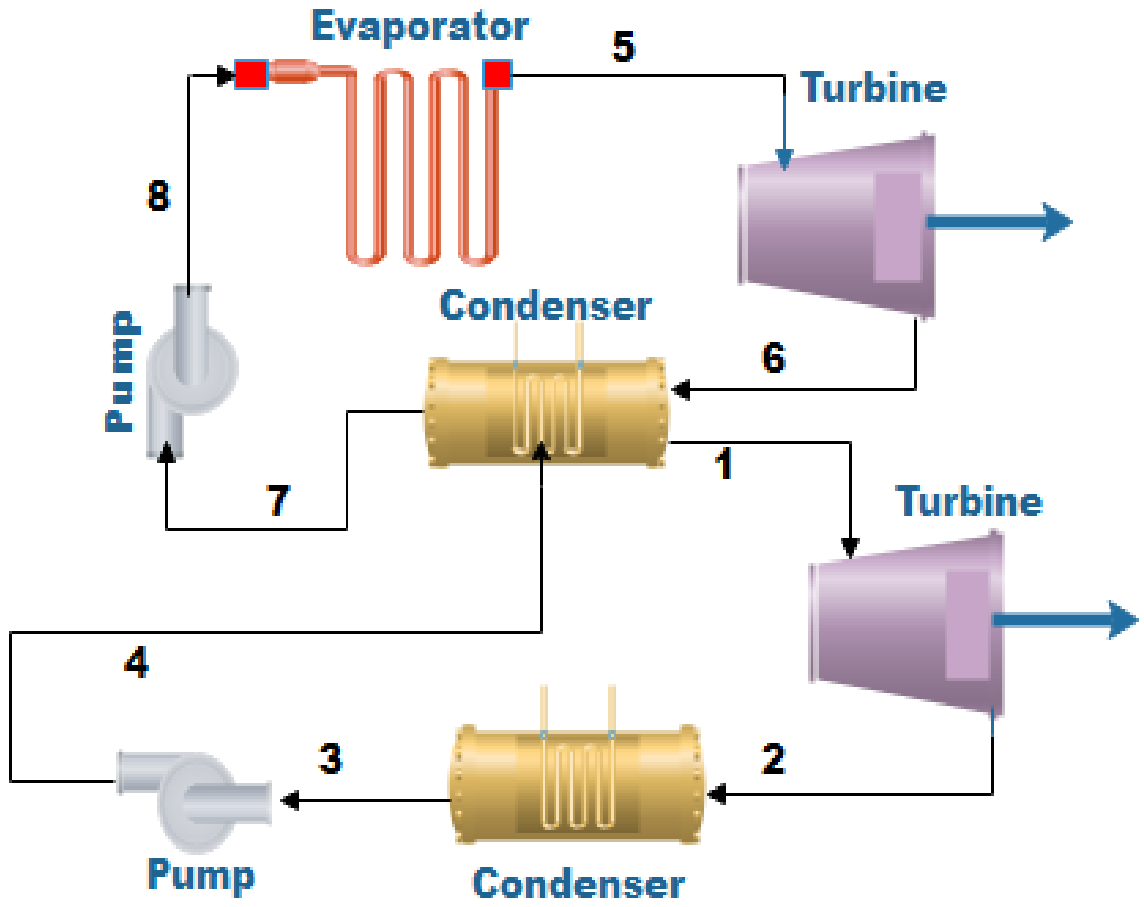

Figure 5 Structure of the CORC.

2.1.6 Regenerative-Superheat Organic Rankine Cycle (RSORC)

This configuration includes a superheater between the evaporator and the turbine of the RORC. The layout is shown in Figure 6.

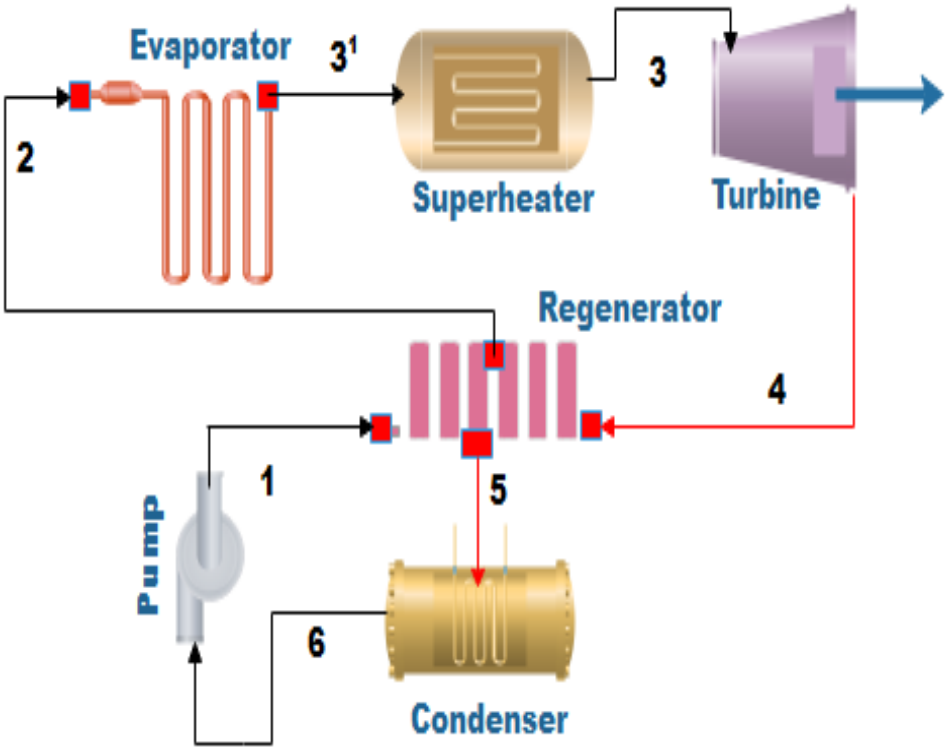

Figure 6 Structure of RSORC.

2.1.7 Regenerative-Reheat Organic Rankine Cycle (RRORC)

This configuration has two turbines and a reheater connected to the RSORC, as shown in Figure 7.

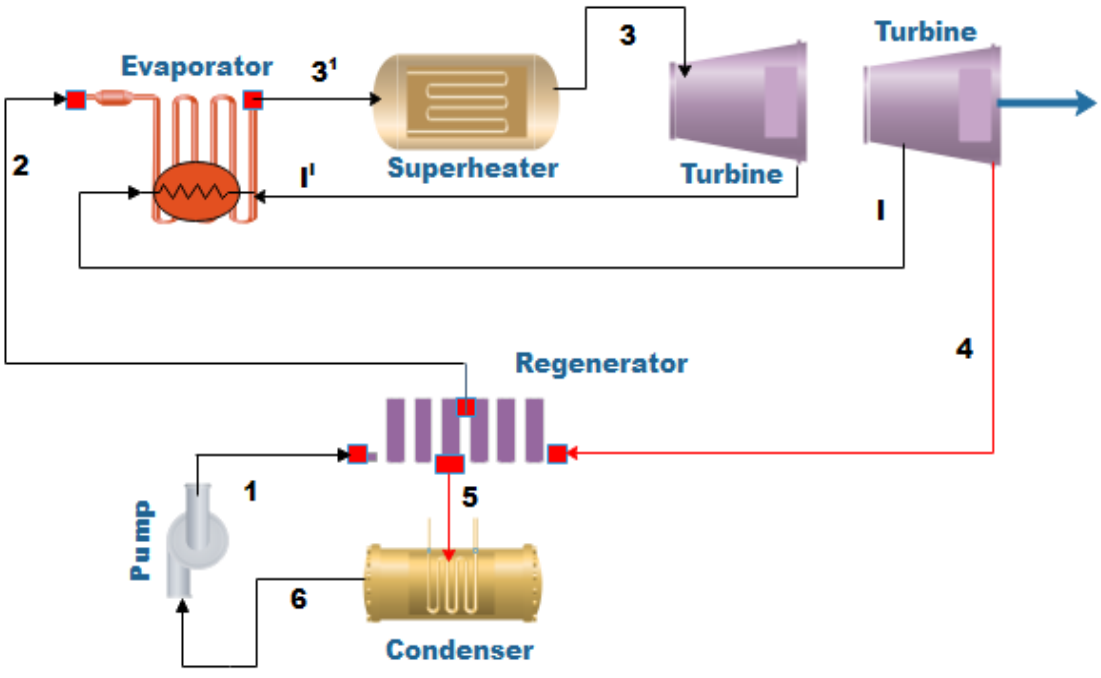

Figure 7 Structure of RRORC.

2.1.8 Two Complementary ORC (2ORC)

This cycle comprises SORC and RORC cycles, as illustrated in Figure 8.

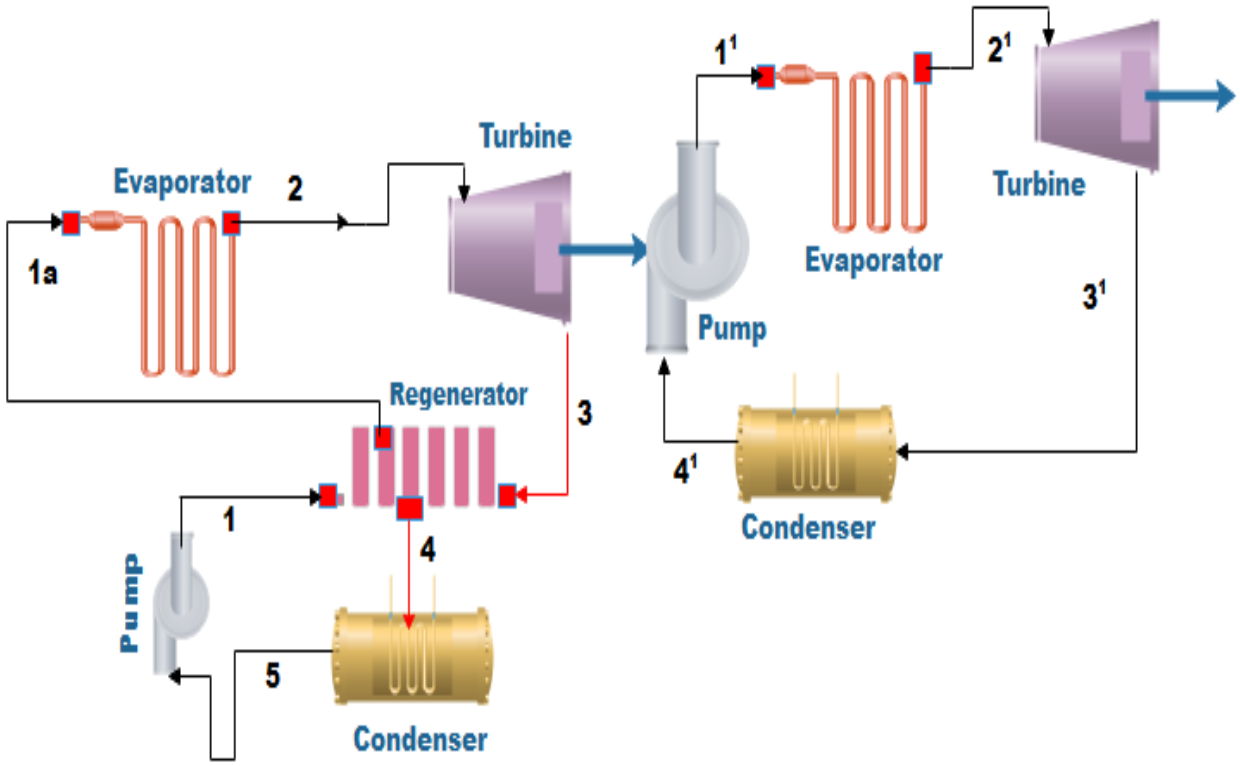

Figure 8 Configuration of 2ORC.

2.2 Thermodynamic Analysis

The thermodynamic procedures presented by Apostol et al. [16], Caceres et al. [23] and Diemuodeke [4] were adopted to formulate the equations for the analysis:

SORC

$$\text{The heat added, } Q_{i,SORC} = m_f(h_3 - h_2) \quad (1)$$

$$\text{The heat rejected, } Q_{o,SORC} = m_f(h_4 - h_1) \quad (2)$$

$$\text{The turbine work output, } W_{T,SORC} = m_f(h_3 - h_4) \quad (3)$$

$$\text{The pump work, } W_{P,SORC} = m_f(h_2 - h_1) \quad (4)$$

$$\text{Thermal efficiency, } \eta_{th,SORC} = \frac{W_T - W_P}{Q_i} \equiv \frac{(h_3 - h_4) - (h_2 - h_1)}{(h_3 - h_2)} \quad (5)$$

ORCS

$$\text{The heat added, } Q_{i,ORCS} = m_f(h_{3'} - h_2) \quad (6)$$

$$\text{The heat rejected, } Q_{o,ORCS} = m_f(h_{4'} - h_1) \quad (7)$$

$$\text{The turbine work output, } W_{T,ORCS} = m_f(h_{3'} - h_4) \tag{8}$$

$$\text{The pump work, } W_{P,ORCS} = m_f(h_2 - h_1) \tag{9}$$

$$\text{Thermal efficiency, } \eta_{th} = \frac{W_T - W_P}{Q_i} \equiv \frac{(h_3{}' - h_4) - (h_{2'} - h_1)}{(h_{3'} - h_2)} \tag{10}$$

ORCSR

$$\text{The heat added, } Q_{i,ORCSR} = m_f(h_{3'} - h_2) + m_f(h_{I'} - h_I) \tag{11}$$

$$\text{The heat rejected, } Q_{o,ORCSR} = m_f(h_{4'} - h_1) \tag{12}$$

$$\text{The turbine work output, } W_{T,ORCSR} = m_f(h_{3'} - h_I) + m_f(h_{I'} - h_{4'}) \tag{13}$$

$$\text{The pump work, } W_{P,ORCSR} = m_f(h_2 - h_1) \tag{14}$$

$$\text{Thermal efficiency, } \eta_{th} = \frac{W_T - W_P}{Q_i} \equiv \frac{(h_{3'} - h_I) + (h_{I'} - h_{4'}) - (h_2 - h_1)}{(h_{3'} - h_2) + (h_{I'} - h_I)} \tag{15}$$

RORC

$$\text{The heat added, } Q_{i,RORC} = m_f(h_{2'} - h_3) \tag{16}$$

$$\text{The heat rejected, } Q_{o,RORC} = m_f(h_5 - h_6) \tag{17}$$

$$\text{The turbine work output, } W_{T,RORC} = m_f(h_3 - h_4) \tag{18}$$

$$\text{The pump work, } W_{P,RORC} = m_f(h_1 - h_6) \tag{19}$$

$$\text{Thermal efficiency, } \eta_{th} = \frac{W_T - W_P}{Q_i} \equiv \frac{(h_3 - h_4) - (h_1 - h_6)}{(h_2 - h_9)} \tag{20}$$

CORC

$$\text{The heat added, } Q_{i,CORC} = (m_{f1}(h_1 - h_4) - \mathcal{E}\left(m_{f2}(h_6 - h_7)\right) + m_{f2}(h_5 - h_8) \tag{21}$$

$$\text{The heat rejected, } Q_{o,CORC} = m_{f1}(h_2 - h_3) \tag{22}$$

$$\text{The turbine work output, } W_{T,CORC} = m_{f1}(h_1 - h_2) + m_{f2}(h_5 - h_6) \tag{23}$$

$$\text{The pump work, } W_{P,CORC} = m_{f1}(h_4 - h_3) + m_{f2}(h_8 - h_7) \tag{24}$$

$$\text{Thermal efficiency, } \eta_{th} = \frac{W_T - W_P}{Q_i} \tag{25}$$

RSORC

$$\text{The heat added, } Q_{i,RSORC} = m_f(h_2 - h_3) \tag{26}$$

$$\text{The heat rejected, } Q_{o,RSORC} = m_f(h_5 - h_6) \tag{27}$$

$$\text{The turbine work output, } W_{T,RSORC} = m_f(h_3 - h_4) \tag{28}$$

$$\text{The pump work, } W_{P,RSORC} = m_f(h_1 - h_6) \tag{29}$$

$$\text{Thermal efficiency, } \eta_{th} = \frac{W_T - W_P}{Q_i} \equiv \frac{(h_3 - h_4) - (h_1 - h_6)}{(h_2 - h_9)} \tag{30}$$

RRORC

$$\text{The heat added, } Q_{i,RRORC} = m_f(h_3 - h_2) + m_f(h_I - h_{I'}) \tag{31}$$

$$\text{The heat rejected, } Q_{o,RRORC} = m_f(h_5 - h_6) \tag{32}$$

$$\text{The turbine work output, } W_{T,RRORC} = m_f(h_3 - h_{I'}) + m_f(h_I - h_4) \tag{33}$$

$$\text{The pump work, } W_{P,RRORC} = m_f(h_1 - h_6) \tag{34}$$

$$\text{Thermal efficiency, } \eta_{th} = \frac{W_T - W_P}{Q_i} \equiv \frac{(h_3 - h_{I'}) + (h_I - h_4) - (h_1 - h_6)}{(h_3 - h_2) + (h_I - h_{I'})} \tag{35}$$

2ORC

$$\text{The heat added, } Q_{i,2ORC} = m_{f1}(h_2 - h_{1a}) + m_{f2}(h_{2'} - h_{1'}) \tag{36}$$

$$\text{The heat rejected, } Q_{o,2ORC} = m_{f1}(h_4 - h_5) + m_{f2}(h_{3'} - h_{4'}) \tag{37}$$

$$\text{The turbine work output, } W_{T,2ORC} = (m_{f1}(h_2 - h_3) - m_{f2}(h_{1'} - h_{4'})) + m_{f2}(h_{2'} - h_{3'}) \tag{38}$$

$$\text{The pump work, } W_{P,2ORC} = m_{f1}(h_1 - h_5) \tag{39}$$

$$\text{Thermal efficiency, } \eta_{th} = \frac{(m_{f1}(h_2 - h_3) - m_{f2}(h_{1'} - h_{4'})) + m_{f2}(h_{2'} - h_{3'}) - m_{f1}(h_1 - h_5)}{m_{f1}(h_2 - h_{1a}) + m_{f2}(h_{2'} - h_{1'})} \tag{40}$$

2.3 Artificial Bee Colony (ABC) Optimization Algorithm

The ABC algorithm consists of four main phases [24]:

i. Initialization Phase

Here, the initial food sources are produced randomly using the expression.

$$x_m = l_i + rand(0,1) * (u_i - l_i) \tag{41}$$

where $u_i \; and \; l_i$ are the upper and lower bound of the solution space of the objective function, and rand (0, 1) is a random number in the range [0, 1].

ii. Employed Bee Phase

The neighbor food source v_{mi} is determined by the following equation.

$$v_{mi} = x_{mi} + \phi_{mi} * (x_{mi} - x_{ki}) \tag{42}$$

where i is a randomly selected parameter index, x_k is a randomly selected food source, ϕ_{mi} is a random number in the range [-1, 1].

The fitness is calculated by applying the following formulae.

$$fit_m(x_m) = \frac{1}{1 + f_m(x_m)} \text{ for } f_m(x_m) > 0 \text{ and} \tag{43}$$

$$fit_m(x_m) = 1 + |f_m(x_m)| \text{ for } f_m(x_m) < 0 \tag{44}$$

where, $f_m(x_m)$ is the objective function value of x_m. After that a greedy selection is applied between x_m and v_m.

iii. Onlooker Bee Phase

The quantity of a food source is evaluated by its profitability and the profitability of all food sources. P_m is determined by the formula.

$$P_m = \frac{fit_m(x_m)}{\sum_{m=1}^{SN} fit_m(x_m)} \tag{45}$$

where, $fit_m(x_m)$ is the fitness of x_m. Onlooker bees search the neighborhoods of food sources according to the expression.

$$v_{mi} = x_{mi} + \phi_{mi} * (x_{mi} - x_{ki}) \tag{46}$$

iv. Scout Phase

The scout bees randomly search the new solutions. The scout will discover the new solution x_m using the expression.

$$x_m = l_i + rand(0,1) * (u_i - l_i) \tag{47}$$

where, rand (0, 1) is a random number within the range [0, 1], $u_i$and l_i are the upper and lower bounds of the solution space of the objective function.

Figure 9 shows the flowchart of the ABC algorithm.

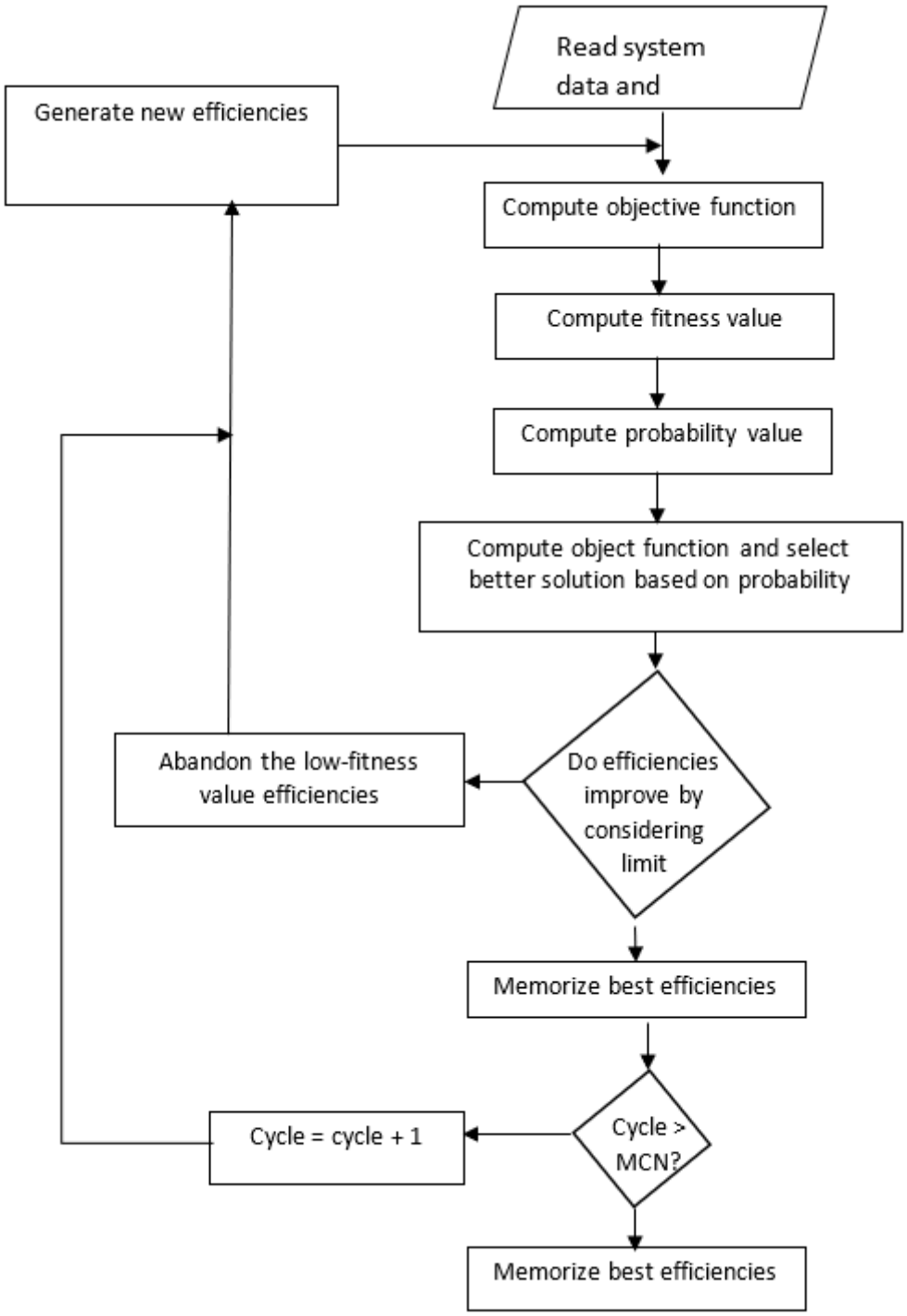

Figure 9 Algorithm for Artificial Bee Colony (ABC).

2.4 Technique for Order Preference by Similarity to Ideal Solution (TOPSIS)

The TOPSIS scheme [25], which allows for the use of intervals to carter for input data range, is described in this section. For an input data of value A in the interval $[a^l, a^u]$, we have

$$A = [a^l, a^u] = \{a | a^l \leq a \leq a^u\} \tag{48}$$

The steps in applying the TOPSIS scheme involve the following:

Step 1: Normalization of Input Data

The normalization uses the vector normalization formula.

$$n_{ij}^{l} = \frac{a_{ij}^{l}}{\sqrt{\sum_{i=1}^{m}\left(\left(a_{ij}^{l}\right)^{2} + \left(a_{ij}^{u}\right)^{2}\right)}} \tag{49}$$

$$n_{ij}^{u} = \frac{a_{ij}^{u}}{\sqrt{\sum_{i=1}^{m}\left(\left(a_{ij}^{l}\right)^{2} + \left(a_{ij}^{u}\right)^{2}\right)}} \tag{50}$$

where n_{ij}^{l}[-] is the normalized lower bound and n_{ij}^{l}[-] is the normalized upper bound of input a_{ij} for an alternative, i and a criteria j; m is the total number of alternatives.

Step 2: Determination of Ideal Solution

An ideal solution is determined for each of the identified alternatives using the following procedure:

i. All alternatives are set in the best situation and the upper bound of the positive ideal is determined using the equation.

$$A_{k}^{+u} = \{v_{1}^{+u}, v_{2}^{+u}, \ldots, v_{n}^{+u}\} = \left\{\left(\max v_{ij}^{u} \,\middle|\, i \in B\right), \left(\min v_{ij}^{l} | i \in C\right)\right\} \tag{51}$$

ii. Determination of the lower bound of the positive solution of an alternative, k, using the equation.

$$\begin{aligned} A_{k}^{+l} &= \{v_{1}^{+l}, v_{2}^{+l}, \ldots, v_{n}^{+l}\} \\ &= \left\{\left(\max\left(\max_{i\neq k}\left(v_{ij}^{u}\right), v_{ij}^{l}\right) \middle| i \in B\right), \left(\min\left(\min_{i\neq k}\left(v_{ij}^{l}\right), v_{ij}^{l}\right) | i \in C\right\}\end{aligned} \tag{52}$$

iii. Determination of upper bound of negative solution.

$$\begin{aligned} A_{k}^{-u} &= \{v_{1}^{-u}, v_{2}^{-u}, \ldots, v_{n}^{-u}\} \\ &= \left\{\left(\min\left(\min_{i\neq k}\left(v_{ij}^{u}\right), v_{kj}^{u}\right) \middle| i \in B\right), \left(\max\left(\max_{i\neq k}\left(v_{ij}^{u}\right), v_{kj}^{l}\right) | i \in C\right\}\end{aligned} \tag{53}$$

iv. Determination of lower bound of negative solution.

$$\begin{aligned} A_{k}^{-l} &= \{v_{1}^{-l}, v_{2}^{-l}, \ldots, v_{n}^{-l}\} \\ &= \left\{\left(\min_{i}\left(v_{ij}^{l}\right) \middle| i \in B\right), \left(\max_{i}\left(v_{ij}^{u}\right) | i \in C\right\}\end{aligned} \tag{54}$$

Step 3: Determination of Euclidean distances

The distances between each alternative and the k[th] ideal alternative are determined as follows:

i. The distance between the worst k[th] alternative and A_{k}^{+u}.

$$d_{k}^{+u} = \sqrt{\sum\nolimits_{j\in B}\left(v_{j}^{+u} - v_{kj}^{l}\right)^{2} + \sum\nolimits_{j\in C}\left(v_{j}^{+u} - v_{kj}^{u}\right)^{2}} \tag{55}$$

ii. The distance between the best k[th] alternative and A_{k}^{+u}

$$d_k^{+l} = \sqrt{\sum_{j\in B}\left(v_j^{+l} - v_{kj}^{u}\right)^2 + \sum_{j\in C}\left(v_j^{+l} - v_{kj}^{l}\right)^2} \tag{56}$$

iii. The distance between the best k[th] alternative and A_k^{-u}.

$$d_k^{-u} = \sqrt{\sum_{j\in B}\left(v_j^{-u} - v_{kj}^{u}\right)^2 + \sum_{j\in C}\left(v_j^{-u} - v_{kj}^{l}\right)^2} \tag{57}$$

iv. The distance between the worst k[th] alternative and A_k^{-u}.

$$d_k^{-l} = \sqrt{\sum_{j\in B}\left(v_j^{-l} - v_{kj}^{l}\right)^2 + \sum_{j\in C}\left(v_j^{-l} - v_{kj}^{u}\right)^2} \tag{58}$$

Step 4: Ranking of alternatives.

Each alternative is assigned a ranked interval, R_k, while the interval function, A, determines the acceptable alternative. They are respectively given by:

$$R_k \in \left[\frac{d_k^{-l}}{d_k^{-u} + d_k^{+u}}, \frac{d_k^{-u}}{d_k^{-l} + d_k^{+l}}\right] = [e^l, e^u] \tag{59}$$

$$A(E < D) = \frac{m(D) - m(E)}{w(D) + w(E)} \tag{60}$$

where $m(D) = \frac{e^l + e^u}{2}$ and $w(D) = \frac{e^l - e^u}{2}$.

Determination of the weights used for TOPSIS is obtained using Analytic Hierarchical Process (AHP) outlined below:

Step 1:

i. Identification of the criteria, m, and formation of matrix $(n \times n)$; $i = 1, 2, \ldots, m$
ii. Assign the numbers; $i, j = 1, 2, \ldots, 9$ in the order of importance of criteria (m) to the project, where the elements in the matrix are characterized in i-th column and j-th row.
iii. Produce the corresponding transpose $j = 1, 2, \ldots, 9$ and insert in $i = 1, 2.., 9$
iv. Generate the rest date in the matrix C, where; $C = C_{ij}$; is the element of the decision matrix residing in the i-th column and j-th row.

Step 2:

i. Obtain the normalize matrix R.

$$R = \{(r_{ij})\} \equiv \frac{x_{ij}}{\sum_{i=1}^{m} x_{ij}} \tag{61}$$

where, $r_{ij} =$ elements of normalized matrix.

ii. Produce the weighted average for each criteria by taking the average in j-th row.

$$w_j = \frac{\sum_{i=1}^{m} r_{ij}}{m} \tag{62}$$

Step 3: Check for correctness of the produced weighted average.

i. $$\text{Obtain } p = \sum_{i=1}^{m} r_{ij} \times w_j \quad (63)$$

ii. $$\text{Obtain } q = \sum p \quad (64)$$

iii. Permissive Error (E) = $CI/RI \leq 0.1$; where $CI = (p-n)/(n-1)$ and RI is obtained from a table based on $'m'$ value.

3. Results and Discussion

3.1 Input Data

The input data to the ABC algorithm include the maximum cycle number (MCN) and other parameters, as shown in Table 1, and the thermodynamic properties of the twelve selected refrigerants, shown in Table 2. In each cycle of the optimization stage, the operating pressures of the condenser and evaporator were varied, and the resultant thermal efficiency was computed. After the optimization, a multi-criteria analysis using the modified TOPSIS scheme was performed. The selected criteria include the environmental and climatic impact of the working fluid with the highest thermal efficiency, the power output, the required heat input to the plant and the power consumed by the pump from the optimization of each configuration.

Table 1 ABC Parameter Values.

Parameter	Value
MCN	1000
Colony Size	6
dimension	4
limit	12

Table 2 Data of working fluids [26].

S/N	Fluid	Molar Mass (kg/kmol)	T_{cr} (°C)	P_{cr} (mPa)	GWP	ODP	Toxicity	Flammability	corrosiveness
1	IsoButane	58.122	151.9	3.79	3	0	no	yes	no
2	R152a	58.122	134.6	3.62	3	0	no	yes	no
3	IsoPentane	17.04	132.2	11.33	0	0	yes	no	yes
4	R134a	137.37	197.9	4.4	4000	1	no	no	no
5	R11	116.95	204.3	4.21	600	0.11	yes	no	no
6	R114	66.051	113.2	4.51	140	0	no	yes	no
7	R113	100.5	137.1	4.05	1800	0.065	yes	yes	no
8	Ethanol	102.03	101.0	4.05	1300	0	no	no	no
9	R142b	46.068	240.7	6.14	n.a	n.a	no	yes	no
10	R141b	187.38	214.0	3.39	6130	1	no	no	no
11	Ammonia	72.149	187.2	3.37	5	0	yes	yes	no
12	nButane	170.92	145.6	3.25	10.04	1	no	no	no

3.2 Results of Thermodynamic Optimization

The thermodynamic-based results were obtained for the various structure of the organic Rankine cycles using the working fluid parameters presented in Table 2 and Table 3 at a mass flowrate of 0.8 kg/s and 40% regenerative heat exchanger effectiveness. Therefore, the results of the thermodynamic optimization based on the ABC algorithm for all the configurations using all twelve working fluids are in Table 4.

Table 3 Condenser and Boiler Pressure Ranges.

S/N	Fluid	Condenser Pressure (Pa)		Boiler Pressure (Pa)	
		min	max	min	max
1	IsoButane	20000	275281.67	275281.67	3.79E+06
2	R152a	20000	269035.31	269035.31	3.62E+06
3	Isopentane	20000	476004.20	476004.2	1.13E+07
4	R134a	20000	296614.23	296614.23	4.40E+06
5	R11	20000	290137.90	290137.9	4.21E+06
6	R114	90000	637032.18	637032.18	4.51E+06
7	R113	20000	284569.85	284569.85	4.05E+06
8	Ethanol	20000	284569.85	284569.85	4.05E+06
9	R142b	20000	350399.77	350399.77	6.14E+06
10	R141b	20000	260345.92	260345.92	3.39E+06
11	Ammonia	20000	259576.58	259576.58	3.37E+06
12	n-Butane	20000	254911.75	254911.75	3.25E+06

Table 4 Optimized thermodynamic parameters.

Structure	Working fluid	Pump Isentropic Eff. nps [-]	Turbine Pressure, [mPa]	Condenser Pressure, [kPa]	Turbine Isentropic Eff [-]	Pump Work, Wp [kW]	Turbine Work, Wt [kW]	Heat Added, Qin [kW]	Heat Rejected, Qout [kW]
SORC	IsoButane	0.60	3.31	90.00	0.90	4.32	96.22	403.30	314.28
	R152a	0.60	3.62	90.00	0.90	2.78	71.54	298.39	231.48
	Isopentane	0.60	3.08	90.00	0.90	3.89	97.09	434.79	344.18
	R134a	0.60	3.64	90.00	0.90	2.05	46.03	202.39	159.77
	R11	0.60	3.89	90.00	0.90	2.04	45.51	184.64	142.53
	R114	0.60	3.09	90.00	0.90	1.57	34.16	154.95	123.42
	R113	0.60	3.00	95.62	0.90	1.54	37.84	174.89	139.61
	Ethanol	0.60	3.93	96.75	0.90	4.16	154.05	755.06	607.94
	R142b	0.60	3.59	90.00	0.90	2.34	53.19	223.43	174.14
	R141b	0.60	3.39	90.00	0.90	2.15	57.52	244.22	190.29
	Ammonia	0.60	3.37	96.49	0.90	3.83	272.46	1144.76	878.69
	n-Butane	0.60	3.25	90.00	0.90	4.18	102.87	436.26	340.36
ORCS	IsoButane	0.6	3.53193	90	0.9	4.61	166.50	592.45	433.64
	R152a	0.6	3.592458	90	0.8924414	2.76	109.95	410.61	305.25
	Isopentane	0.6	3.37	90	0.9	4.26	168.70	633.95	472.36
	R134a	0.6	4	90	0.9	2.26	79.44	294.93	219.26
	R11	0.6	4.21	90	0.9	2.22	69.07	246.96	181.58
	R114	0.6	3.21	90	0.9	1.63	58.47	224.08	168.33
	R113	0.6	3.3	93.06	0.9	1.69	61.53	241.85	183.14
	Ethanol	0.6	4.05	90	0.9	4.28	215.18	952.37	744.33
	R142b	0.6	4	90	0.9	2.61	87.92	316.20	232.62
	R141b	0.6	3.39	96.659	0.9	2.15	83.56	320.69	240.72

	Ammonia	0.6	3.35	90	0.9	3.81	340.09	1342.49	1008.75
	n-Butane	0.6	3.193806	90	0.9	4.11	166.85	616.93	456.92
ORCSR	IsoButane	0.6	3.6	90	0.9	4.70	360.52	853.65	500.96
	R152a	0.6	3.62	137.994	0.9	2.80	183.86	532.43	353.23
	Isopentane	0.6	3.37	90	0.9	4.26	400.38	928.33	535.05
	R134a	0.6	4	103.141	0.9	2.27	150.41	401.48	254.85
	R11	0.6	4.21	90	0.9	2.22	125.79	337.71	215.62
	R114	0.6	3.21	90	0.9	1.63	129.51	318.79	192.00
	R113	0.6	2.905991	90	0.9	1.49	133.69	337.32	206.11
	Ethanol	0.6	4.05	90	0.9	4.28	351.46	1202.58	858.27
	R142b	0.6	3.852419	90	0.9	2.51	169.01	436.86	272.03
	R141b	0.6	3.39	113.779	0.9	2.16	162.91	435.17	275.86
	Ammonia	0.6	3.37	93.827	0.9	3.83	399.46	1578.16	1185.09
	n-Butane	0.6	3.25	102.483	0.9	4.19	355.46	870.65	522.17
RORC	IsoButane	0.6	2.624545	90	0.8900267	3.40	93.62	396.04	321.97
	R152a	0.6	3.62	90	0.9	2.78	71.64	298.72	231.71
	Isopentane	0.6	3.077625	98.526	0.9	3.89	94.72	397.10	342.61
	R134a	0.6	3.498377	90	0.9	1.97	46.47	204.83	161.64
	R11	0.6	4.013514	90	0.9	2.11	45.30	183.30	141.52
	R114	0.6	2.927619	90	0.9	1.49	34.49	149.28	124.92
	R113	0.6	3.006701	90	0.9	1.54	38.59	164.39	140.37
	Ethanol	0.6	4.05	90	0.9	4.28	157.49	758.40	608.05
	R142b	0.6	3.709237	90	0.9	2.41	52.93	221.81	172.90
	R141b	0.6	3.39	90	0.9	2.15	57.58	238.93	190.42
	Ammonia	0.6	3.37	90	0.9	3.83	276.95	1150.00	879.43
	n-Butane	0.6	3.170704	90	0.9	4.08	102.94	422.30	341.57
CORC	IsoButane	0.6	3.6	90	0.9	9.41	298.30	933.56	406.83
	R152a	0.6	3.62	90	0.9	5.56	201.45	653.09	288.06

	Isopentane	0.6	3.37	90	0.9	8.53	300.21	994.27	442.66
	R134a	0.6	3.892519	90	0.9	4.39	141.37	464.33	206.43
	R11	0.6	4.21	90	0.9	4.43	126.89	396.50	173.12
	R114	0.6	3.193368	90	0.9	3.25	104.57	352.80	158.53
	R113	0.6	3.3	90	0.9	3.39	112.22	384.33	173.59
	Ethanol	0.6	4.05	90.297	0.9	8.57	399.04	1524.98	712.64
	R142b	0.6	3.911231	90	0.9	5.10	157.83	500.83	219.69
	R141b	0.6	3.39	90	0.8938695	4.30	154.06	514.40	229.70
	Ammonia	0.6	3.37	90	0.9	7.66	645.78	2198.45	978.40
	n-Butane	0.6	3.25	90	0.9	8.36	299.99	973.27	429.51
RSORC	IsoButane	0.6	3.6	96.366	0.9	4.71	165.07	520.51	433.61
	R152a	0.6	3.62	90.353	0.9	2.78	111.02	391.41	304.30
	Isopentane	0.6	3.37	90	0.9	4.26	168.70	536.12	472.36
	R134a	0.6	4	90	0.9	2.26	79.44	272.76	219.26
	R11	0.6	4.195337	90	0.9	2.21	69.01	229.14	181.58
	R114	0.6	3.21	90	0.8963921	1.63	58.24	194.60	168.57
	R113	0.6	3.3	90.908	0.9	1.69	61.87	208.85	183.32
	Ethanol	0.6	4.05	90	0.9	4.28	215.18	921.97	744.33
	R142b	0.6	4	90	0.8954393	2.61	87.48	289.62	233.07
	R141b	0.6	3.39	90	0.9	2.15	84.94	291.67	241.20
	Ammonia	0.6	3.33	90	0.9	3.78	339.50	1342.32	1009.13
	n-Butane	0.6	3.25	90	0.9	4.18	167.84	544.96	457.44
RRORC	IsoButane	0.6	3.6	90	0.9	4.70	360.52	750.26	500.96
	R152a	0.6	3.62	95.049	0.9	2.78	193.54	500.64	358.53
	Isopentane	0.6	3.37	90	0.9	4.26	400.38	799.16	535.05
	R134a	0.6	3.99714	90	0.9	2.26	153.05	364.87	256.25
	R11	0.6	4.21	90	0.9	2.22	125.79	302.93	215.62
	R114	0.6	3.21	90	0.9	1.63	129.51	277.59	192.00

	R113	0.6	3.3	90	0.9	1.69	138.85	298.70	208.98
	Ethanol	0.6	4.015836	90	0.9	4.25	350.64	1114.28	857.90
	R142b	0.6	3.967692	90	0.9	2.59	170.35	392.33	272.67
	R141b	0.6	3.331648	90	0.9	2.11	168.09	393.45	278.33
	Ammonia	0.6	3.37	90	0.9	3.83	401.82	1539.06	1186.24
	n-Butane	0.6	3.25	90	0.9	4.18	362.14	772.90	524.70
2ORC	IsoButane	0.6	3.314855	90	0.9	4.32	188.63	797.84	314.80
	R152a	0.6	3.62	90	0.8733816	2.78	136.27	597.44	233.82
	Isopentane	0.6	3.134489	90	0.9	3.96	190.37	835.13	343.76
	R134a	0.6	2.959688	90	0.9	1.66	91.27	418.93	165.77
	R11	0.6	3.937721	90	0.9	2.07	88.90	368.54	142.24
	R114	0.6	3.005086	90	0.9	1.53	67.32	305.15	124.39
	R113	0.6	3.071542	90	0.9	1.57	75.54	339.99	139.96
	Ethanol	0.6	4.05	100.653	0.9	4.29	302.17	1503.70	605.77
	R142b	0.6	3.655734	90	0.9	2.38	103.87	445.56	173.62
	R141b	0.6	3.39	90	0.9	2.15	113.01	483.34	190.42
	Ammonia	0.6	3.37	90	0.9	3.83	550.07	2299.99	879.43
	n-Butane	0.6	3.25	90	0.9	4.18	201.88	858.58	340.72

Figure 10 shows the variation of thermal efficiency with the various ORC structures and the twelve working fluids. The figures show that RRORC and SORC structures have the best and the worst thermal performance, respectively.

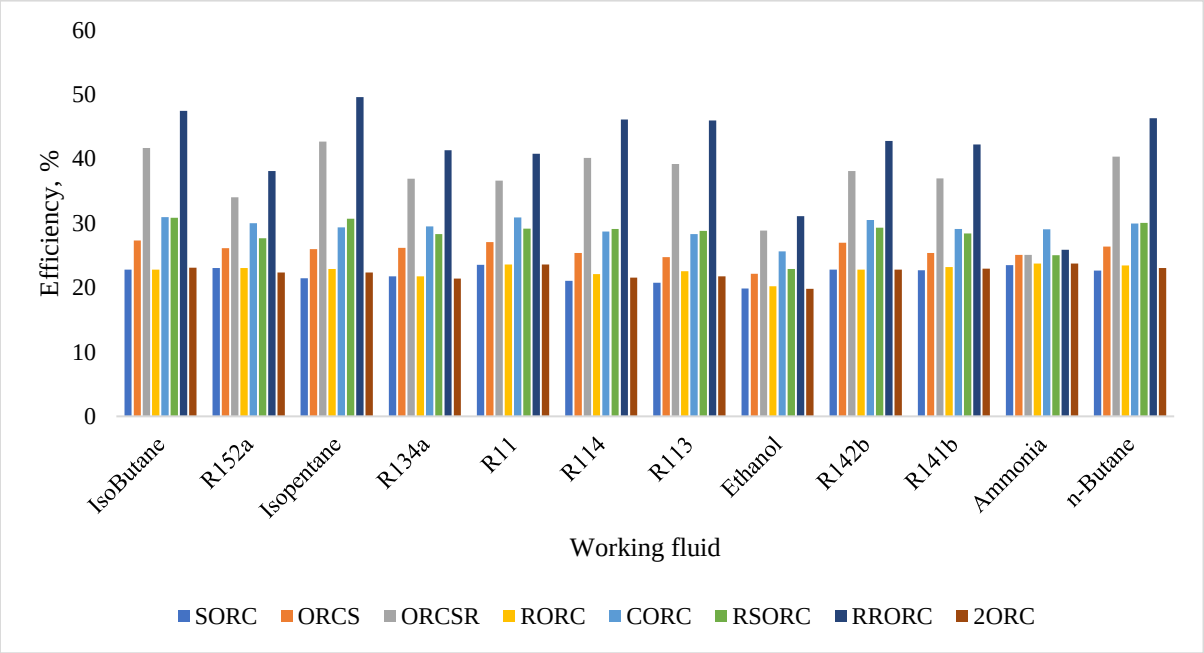

Figure 10 Thermal Efficiency.

3.3 Results of Structural Optimization

All twelve working fluids used for the optimization and the corresponding optimum thermal efficiencies, work output, pump work and the environmental impact of the working fluids are then inputted into the TOPSIS algorithm. Subsequently, the modified TOPSIS scheme was applied, coupled with the weights determined from the AHP algorithm, where the relative importance is assigned to the criteria. The obtained weights are presented in Table 5. The TOPSIS scheme for selecting the best configuration is presented in Table 6. The detailed results from the modified TOPSIS analysis are presented in Table S1 in the Appendix, showing the cost (C) and benefits (B) for various parameters of interest. The observed output indicated a selection of RRORC at indicated weights, while SORC resulted in the least in selection ranking. The RRORC has the following performance; thermal efficiency of 49.5%, maximum power output of 0.4 MW, condenser pressure of 90 kPa, and turbine pressure of 3.37 MPa.

Table 5 AHP Weights for TOPSIS.

Criteria	Weight	Direction of optimization
Thermal Efficiency (-)	0.20107	Max
ODP (-)	0.15027	Min
Turbine pressure (-)	0.13148	Min
Condenser Pressure (-)	0.17531	Min
Power output (-)	0.13148	Max
GWP (-)	0.21038	Min

Table 6 TOPSIS Ranking.

e^l	e^u	Mid Point	Half width	Rank
0.0092	0.6101	0.3096	0.3005	8
0.54	0.8522	0.6961	0.1561	6
0.7758	0.9217	0.8488	0.0729	2
0.535	0.8498	0.6924	0.1574	7
0.5548	0.9348	0.7448	0.19	3
0.5397	0.8741	0.7069	0.1672	5
0.7704	0.9378	0.8541	0.0837	1
0.5381	0.897	0.7175	0.1795	4

4. Conclusion

In response to the Paris Agreement, reached in 2015, many nations have begun to chart development pathways away from climate-forcing activities; where the oil and gas sector dominates in the energy space. Therefore, are ambitious medium- to long-term plans to rapidly introduce low/zero energy conversion technologies into the energy generation space, renewable energy technologies. Therefore, this work presents the thermodynamics and structural optimizations of different organic Rankine cycle structures, which are well aligned with biomass-to-power technology. This project considered eight (8) configurations of the Organic Rankine Cycle, which include the Simple Organic Rankine Cycle (SORC), Regenerative Organic Rankine Cycle (RORC), Cascade Organic Rankine Cycle (CORC), Organic Rankine Cycle with Superheat (ORCS) and Organic Rankine Cycle with Superheat and Reheat (ORCSR), Regenerative Superheat ORC, Regenerative Reheat ORC and 2ORC. The artificial bee colony algorithm was used to conduct the thermodynamic optimization, whereas the modified TOPSIS multi-criteria decision-making was used to conduct the structural configuration. The criteria of interest under the modified TOPSIS were the Global Warming Potential, Ozone Depletion Potential, compressor power input, turbine power output and the thermal efficiency of the configuration. The overall optimization study shows that RRORC, operating with an isopentane of 0 GWP and ODP, was selected as the best ORC configuration. The RRORC has the following performance; thermal efficiency of 49.5%, maximum power output of 0.4 MW, condenser pressure of 90 kPa, and turbine pressure of 3.37 MPa. The results presented in this work will support clean energy developers in the clean energy access sector, especially in the agrarian community with huge agro-waste generation potentials. Future work is expected to apply the optimal system to develop agro-waste fired combined heat and power system to provide a clean energy system for agrarian communities that currently have limited access to modern energy supply.

Author Contributions

ADU was responsible for data collection, model formulation, simulation, result interpretation and first darft manuscript, OED conceived and supervised the project, reviewed models and proof read manuscript, MMO co-supervised the project, reviewed models and proof read final manuscript, FIA was responsible for process diagram, model review, interpretation of results and proof reading

of manuscript and JCO was responsible for data curation, model review, interpretation of results and proof reading of manuscript.

Competing Interests

The authors have declared that no competing interests exist.

Additional Materials

The following additional materials are uploaded at the page of this paper.

1. Table S1: TOPSIS Implementation for the Selection of the Best Configuration.

References

1. Ryder SS. Developing an intersectionally-informed, multi-sited, critical policy ethnography to examine power and procedural justice in multiscalar energy and climate change decisionmaking processes. Energy Res Soc Sci. 2018; 45: 266-275.
2. Liang Y, Kleijn R, Tukker A, van der Voet E. Material requirements for low-carbon energy technologies: A quantitative review. Renew Sustain Energy Rev. 2022; 161: 112334.
3. Giwa A, Alabi A, Yusuf A, Olukan T. A comprehensive review on biomass and solar energy for sustainable energy generation in Nigeria. Renew Sustain Energy Rev. 2017; 69: 620-641.
4. Diemuodeke OE, Mulugetta Y, Imran M. Techno-economic and environmental feasibility analysis of rice husks fired energy system for application in a cluster of rice mills. Renew Sustain Energy Rev. 2021; 149: 111365.
5. Penh P. Task 3: Markets, policies and institutions. Feasibility study of renewable energy options for rural electrification in Cambodia (REOREC). 2006. EuropeAid/119920/C/SV.
6. Wood IP, Cao HG, Tran L, Cook N, Ryden P, Wilson DR, et al. Comparison of saccharification and fermentation of steam exploded rice straw and rice husk. Biotechnol Biofuels. 2016; 9: 193.
7. Park BS, Usman M, Imran M, Pesyridis A. Review of organic Rankine cycle experimental data trends. Energy Convers Manag. 2018; 173: 679-691.
8. Aboelwafa O, Fateen SEK, Soliman A, Ismail IM. A review on solar Rankine cycles: Working fluids, applications, and cycle modifications. Renew Sust Energ Rev. 2018; 82: 868-885.
9. Preißinger M, Heberle F, Brüggemann D. Thermodynamic analysis of double-stage biomass fired organic Rankine cycle for micro-cogeneration. Int J Energy Res. 2012; 36: 944-952.
10. Zhang FY, Feng YQ, He ZX, Xu JW, Zhang Q, Xu KJ. Thermo-economic optimization of biomass-fired organic Rankine cycles combined heat and power system coupled CO_2 capture with a rated power of 30 kW. Energy. 2022; 254: 124433.
11. Pezzuolo A, Benato A, Stoppato A, Mirandola A. Fluid selection and plant configuration of an ORC-biomass fed system generating heat and/or power. Energy Procedia. 2016; 101: 822-829.
12. Pode R, Pode G, Diouf B. Solution to sustainable rural electrification in Myanmar. Renew Sust Energ Rev. 2016; 59: 107-118.
13. Strzalka R, Schneider D, Eicker U. Current status of bioenergy technologies in Germany. Renew Sust Energ Rev. 2017; 72: 801-820.

14. Arafat HA, Jijakli K. Modeling and comparative assessment of municipal solid waste gasification for energy production. Waste Manage. 2013; 33: 1704-1713.
15. Apostol V, Pop H, Dobrovicescu A, Prisecaru T, Alexandru A, Prisecaru M. Thermodynamic analysis of ORC configurations used for WHR from a turbocharged diesel engine. Procedia Eng. 2015; 100: 549-558.
16. Hussain D, Sharma M, Shukla AK. Investigative analysis of light duty diesel engine through dual loop organic Rankine cycle. Mater Today. 2021; 38: 146-152
17. Ebrahimi K, Jones GF, Fleischer AS. The viability of ultra low temperature waste heat recovery using organic Rankine cycle in dual loop data center applications. Appl Therm Eng. 2017; 126: 393-406.
18. McMahan AC. Design & optimization of organic Rankine cycle solar-thermal powerplants. Madison, Wisconsin: University of Wisconsin-Madison; 2006.
19. Saffari H, Sadeghi S, Khoshzat M, Mehregan P. Thermodynamic analysis and optimization of a geothermal Kalina cycle system using artificial bee colony algorithm. Renew Energ. 2016; 89: 154-167.
20. Sun X. Multiple criteria decision analysis techniques in aircraft design and evaluation processes. Hamburg, Germany: Technische Universität Hamburg; 2012.
21. Wang JJ, Jing YY, Zhang CF, Shi GH, Zhang XT. A fuzzy multi-criteria decision-making model for trigeneration system. Energy Policy. 2008; 36: 3823-3832.
22. Garcia-Saez I, Méndez J, Ortiz C, Loncar D, Becerra JA, Chacartegui R. Energy and economic assessment of solar Organic Rankine Cycle for combined heat and power generation in residential applications. Renew Energy. 2019; 140: 461-476
23. Cáceres IE, Agromayor R, Nord LO. Thermodynamic optimization of an organic Rankine cycle for power generation from a low temperature geothermal heat source. Proceedings of the 58th Conference on Simulation and Modelling (SIMS 58); 2017 September 25-27; Reykjavik, Iceland.
24. Ullah K, Jiang Q, Geng G, Rahim S, Khan RA. Optimal power sharing in microgrids using the artificial bee colony algorithm. Energies. 2022; 15: 1067.
25. Streimikiene D, Baležentis T. Multi-criteria assessment of small scale CHP technologies in buildings. Renew Sust Energ Rev. 2013; 26: 183-189.
26. Vanderplaats GN. Structural optimization for statics, dynamics and beyond. J Braz Soc Mech Sci Eng. 2006; 28: 316-322.